Article:
Panagi, Marios, Sommariva, Roberto, Fleming, Zoë L. et al. (2026) Daily evolution of VOCs in Beijing: chemistry, emissions, transport, and policy implications. Atmospheric Pollution Research. 102783. ISSN: 1309-1042

https://doi.org/10.1016/j.apr.2025.102783

Atmospheric Pollution Research 17 (2026) 102783

Contents lists available at ScienceDirect

Atmospheric Pollution Research

journal homepage: www.elsevier.com/locate/apr

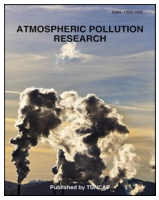

Daily evolution of VOCs in Beijing: chemistry, emissions, transport, and policy implications

Marios Panagi [a,b,m,*], Roberto Sommariva [c], Zoë L. Fleming [d], Paul S. Monks [a], Gongda Lu [c], Eloise A. Marais [e], James R. Hopkins [f,g], Alastair C. Lewis [f,g], Qiang Zhang [h], James D. Lee [f], Freya A. Squires [g,n], Lisa K. Whalley [i], Eloise J. Slater [j], Dwayne E. Heard [j], Robert Woodward-Massey [k], Chunxiang Ye [k], Joshua D. Vande Hey [b,l]

[a] Department of Chemistry, University of Leicester, Leicester, UK
[b] Department of Physics and Astronomy, Earth Observation Science Group, University of Leicester, Leicester, UK
[c] School of Geography, Earth and Environmental Sciences, University of Birmingham, Birmingham, UK
[d] Centro de Investigación en Tecnologías para la Sociedad, Facultad de Ingeniería, Universidad del Desarrollo, Santiago, Chile
[e] Department of Geography, University College London, London, UK
[f] National Centre for Atmospheric Science, University of York, York, UK
[g] Wolfson Atmospheric Chemistry Laboratories, University of York, York, UK
[h] Ministry of Education Key Laboratory for Earth System Modeling, Tsinghua University, Beijing, China
[i] National Centre for Atmospheric Science, School of Chemistry, University of Leeds, Leeds, UK
[j] School of Chemistry, University of Leeds, Leeds, UK
[k] Beijing Innovation Centre for Engineering Science and Advanced Technology, Peking University, Beijing, China
[l] Centre for Environmental Health and Sustainability, University of Leicester, Leicester, UK
[m] Now at Climate and Atmosphere Research Center, The Cyprus Institute, Nicosia, 2121, Cyprus
[n] Now at British Antarctic Survey, Natural Environment Research Council, Cambridge, CB3 0ET, UK

ARTICLE INFO

Keywords:
Volatile organic compounds (VOCs)
Atmospheric chemistry
Ozone formation potential (OFP)
NAME dispersion model
AtChem2 box model

ABSTRACT

Volatile organic compounds (VOCs) are important precursors to the formation of ozone (O_3) and secondary organic aerosols (SOA) and can also have direct human health impacts. The emissions of VOCs remain poorly characterized due to the complexity and variability of their sources. The VOC levels in Beijing during the winter campaign (APHH) were investigated using a dispersion model (NAME), and a chemical box model (AtChem2) in order to understand how chemistry and transport affect the VOC concentrations in Beijing. Emissions of VOCs in Beijing and contributions from outside Beijing were modelled using the NAME dispersion model combined with the emission inventories and were used to initialize the AtChem2 box model. The modelled concentrations of VOCs from the NAME-AtChem2 combination were then compared to the output of a chemical transport model (GEOS-Chem). The results from the emission inventories and the NAME air mass pathways suggest that industrial sources to the south of Beijing and within Beijing during the winter campaign are very important in controlling the VOC levels in Beijing. A number of scenarios with different nitrogen oxides to ozone ratios (NO_x/O_3) and hydroxyl (OH) levels were simulated to determine the changes in VOC levels. In Beijing over 80 % of VOC are emitted locally during winter. Most scenarios are in good agreement with daily GEOS-Chem simulations, with the best agreements seen for the modelled concentrations of ethanol, benzene and propane with correlation coefficients of 0.67, 0.63 and 0.64 respectively. Furthermore, the production of formaldehyde in an air mass within 24 h of travel from Beijing was investigated, and it was estimated that 90 % of formaldehyde in Beijing is secondary, produced from oxidation of non-methane volatile organic compounds (NMVOCs). The benzene/CO and toluene/CO ratios during the campaign are very similar to the ratio derived from literature for 2014 in Beijing, however more data are needed to enable investigation of more species over longer timeframes to determine whether this ratio can be applied to predicting VOCs in Beijing. The results suggest that VOC concentrations in Beijing are driven predominantly by sources within Beijing and by local atmospheric chemistry

* Corresponding author. Department of Physics and Astronomy, Earth Observation Science Group, University of Leicester, Leicester, UK.
E-mail address: mp670@le.ac.uk (M. Panagi).

https://doi.org/10.1016/j.apr.2025.102783
Received 14 March 2025; Received in revised form 10 October 2025; Accepted 10 October 2025
Available online 14 October 2025

during the winter. Moreover, the relationship of the NO_x/VOC and O_3 shows that the VOCs during the winter campaign are possibly emitted from similar sources as NO_x.

1. Introduction

Volatile organic compounds (VOCs) are reactive chemicals emitted from a variety of anthropogenic sources such as vehicles, industry, and solvents, as well as from biogenic sources. VOCs are important precursors to the formation of secondary pollutants and can form pollutants such as secondary organic aerosol (SOA) and ozone (O_3) through photochemical reactions with nitrogen oxides ($NO_x = NO + NO_2$) (Carter and Seinfeld, 2012; Atkinson, 2000; Monks et al., 2009, 2015). Exposure to O_3 pollution can lead to adverse health effects such as lung inflammation and airway hyperactivity (Uysal and Schapira, 2003; Liu et al., 2018). Ozone production depends on the relative abundance of VOCs and NOx. In high-NOx (VOC-limited) environments, ozone formation increases with VOCs, whereas in low-NOx (NOx-limited) environments, it increases with NOx (Sillman, 1999). The VOC/NO_x ratio is therefore very important in order to understand the ozone formation potential and develop policies to reduce O_3 concentrations (LaFranchi et al., 2011). Additionally, human exposure to some VOCs at elevated ambient levels has been associated with adverse health outcomes. For example, formaldehyde is known to induce acute poisoning and is a probable carcinogen, while benzene and other traffic-related VOCs could cause respiratory effects by irritating the airways (Rumchev et al., 2007; Tang et al., 2009).

Previous work has shown that during winter, biofuel and coal burning are significant sources of VOCs in Beijing (Liu et al., 2016; Zhang et al., 2016). For example, Gu et al. (2019) studied the presence of 99 non-methane VOCs (NMVOCs) in Beijing during winter and summer. They found that the concentrations of total NMVOCs were highest on the winter polluted days, followed by the summer polluted days, then the summer normal (i.e., less polluted) days, and the least polluted on the winter normal days. On the other hand, the oxygenated volatile organic compounds (OVOCs) were the highest on the summer polluted days, followed by the summer normal days, then the winter polluted days, and least polluted on the winter normal days.

Yao et al. (2015) determined from studying 18 different sized diesel trucks that carbonyls, aromatics, and alkanes were the dominant species emitted, with carbonyls accounting for 43–69 % of the total VOCs emitted. Yang et al. (2018) determined that VOC levels decreased approximately 50 % during an enhanced emission control period, where all emission sectors were controlled except for the residential sector. Furthermore, they observed that during the study period, all observed high VOC episodes in Beijing occurred during southerly winds indicating the effect of the meteorology and the influence of the heavily industrialized regions to the south of the city.

In megacities where motor vehicles can be the dominant sources of air pollution, the VOCs and carbon monoxide (CO) emissions are highly correlated due to co-emissions and therefore, by using the VOC/CO enhancement ratios, it is possible to predict the VOC levels and their speciation (Parrish et al., 2009; Warneke et al., 2012). Similarly, von Schneidemesser et al. (2010) determined that there were similar reductions in both CO and VOCs in London during the period 1998 to 2007 and for the majority of species the VOC/CO ratios remained steady over the study period.

A number of modelling studies have looked into policy controls to reduce ozone. Using the GEOS-Chem chemical transport model (CTM) it has been postulated that the $PM_{2.5}$ decrease in China results in increases in O_3 owing to the slowing down of reactive uptake in HO_2 and NO_x from aerosols and the need for VOC controls to reduce ozone and offset the effect of the PM_2.5 decrease (Wang et al., 2013; K. Li et al., 2019; K. Li et al., 2019). The emission inventories that are used in chemical transport models are vital for informing policies, but there are many discrepancies among different emission inventories such as underestimations of VOCs and emerging sources for oxygenated VOCs (OVOCs) (Saikawa et al., 2017; Karl et al., 2018; McDonald et al., 2018).

The objective of this study is to determine what controls VOC levels in Beijing, the effects on VOC levels under different scenarios, and how they affect ozone formation potential. Furthermore, the relationship of the NO_x/VOC of the measured VOCs and the modelled VOCs is investigated. Approaches used include: analysis of VOC/CO ratios, using the NAME dispersion model to investigate air mass pathways and transportation of VOCs, using NAME coupled with the AtChem2 box model to investigate how chemistry can affect VOC levels, and use of a CTM (GEOS-Chem). Only emissions that are within the 1-day backward footprints were considered, in order to focus on the immediate contributions from within Beijing and nearby regions outside of Beijing. The measurements analysed here were taken during the 2016 APHH-Beijing campaign, and although recent multi-year analyses show substantial VOC reductions in Beijing, the overall source profile remains persistent —dominated by vehicle, solvent, and combustion emissions—in a largely VOC-limited photochemical regime (Li et al., 2023; Liu et al., 2023, 2024; Cui et al., 2022). The aim of this study is to investigate how emission sources, transport, and chemical processing influence VOC levels and variability, using the 2016 APHH-Beijing dataset as a case study.

2. Methods

2.1. In situ measurements

VOCs were measured in situ during the Air Pollution and Human Health (APHH-Beijing) winter campaign (10 November–10 December 2016) at the Institute of Atmospheric Physics (IAP) tower (39.975° N, 116.377° E), located in the city centre of Beijing between two major ring roads. The measurements followed the protocols described in Shi et al. (2019), who detail the instrumentation, calibration, and data quality control used across the coordinated campaign. The VOC dataset included observations from dual-channel gas chromatography with flame ionization detectors (DC-GC-FID; Hopkins et al., 2011), complemented by proton-transfer-reaction mass spectrometry (PTR–MS). Instruments were calibrated using certified gas standards, with regular zero and span checks performed throughout the campaign. As reported by Shi et al. (2019), measurement precision for VOC species was typically within 5 %. Formaldehyde (HCHO) was measured by laser-induced fluorescence spectroscopy (LIF; Cryer, 2016; Slater et al., 2020; Whalley et al., 2021). Associated radical and reactivity measurements were performed using the Fluorescence Assay by Gas Expansion (FAGE) instrument, as described by Whalley et al. (2021). The FAGE instrument was calibrated every three days, and the overall uncertainty in measured OH and HO_2 concentrations was approximately ±26 % (2σ). Calibration and data acquisition procedures for VOCs and radicals were coordinated within the APHH project, and the combined dataset underwent centralized QA/QC screening before analysis. CO measurements at the IAP site were made using six clustered electrochemical sensors (Alphasense Ltd.) in a 2 × 3 formation. O_3, NO, and NO_2 were measured with commercial instruments (TEI 49i, TEI 42i, and Teledyne CAPS, respectively; Shi et al., 2019).

2.2. The NAME dispersion model

The air mass pathways arriving at Beijing during the study period were modelled using the Numerical Atmospheric Modelling Environment (NAME) model created by the Met Office UK (Jones et al. 2007).

NAME uses meteorological fields from the Unified Model (Brown et al., 2012), to track the pathways of inert tracers. These fields during our study period have a resolution of 0.23°longitude by 0.16°latitude with 59 vertical levels up to an approximate height of 30 km.

For this study, 3-hourly footprints are modelled by 1-day backwards runs with a resolution of 0.25°x 0.25°of all air masses in a layer from 0 to 100 m above ground from 10th of November 2016 to 30th of November 2016. The modelled NAME footprints are combined with gas emission inventories to calculate the mixing ratio of the species at the measurement site (Oram et al., 2017; Panagi et al., 2020) (Fig. 1).

2.3. The AtChem2 atmospheric chemistry box model

AtChem2 (Sommariva et al., 2019) is a box model for atmospheric chemistry designed to use the Master Chemical Mechanism (MCM). In this study, since there is no chemistry involved in the mixing ratios modelled from the combination of NAME footprints with the emission inventories, the AtChem2 box model was used to estimate the impacts of chemical processes on the emitted VOCs. A subset of the MCM was used, including only inorganic reactions, methane (CH_4) reactions and the reactions of the VOCs being investigated. The framework of AtChem2 combined with NAME dispersion footprints is illustrated in Fig. 2.

2.4. The GEOS-Chem chemical transport model

To place the outputs of this novel modelling approach within a regional context, a chemical transport model (CTM) was employed for the winter case study. CTMs operate at coarser spatial resolutions than dispersion models but integrate meteorology with gas- and aerosol-phase chemistry, providing a broader understanding of the limitations and representativeness of the combined NAME-AtChem2 framework. Surface VOC concentrations over China coincident with the APHH-Beijing campaign in November 2016 were simulated using the GEOS-Chem CTM version 12.0.0 nested over East Asia (11° S–55° N, 60–150° E) at 0.5° × 0.625° horizontal resolution. The model includes detailed tropospheric HOx–NOx–VOC–O3–aerosol chemistry and is driven by MERRA-2 meteorological reanalysis data. Anthropogenic emissions for China are taken from the MEIC inventory (Li et al., 2017; Zheng et al., 2018), while other relevant regional sources include biomass burning (Giglio et al., 2013), biogenic VOCs (Guenther et al., 2012), and soil NOx (Hudman et al., 2012). The model was spun up for two months prior to analysis, and daily 24-h mean surface concentrations of seven VOCs (benzene, toluene, ethane, propane, acetone, formaldehyde, and ethanol) were extracted for November 2016. These were compared with the NAME-AtChem2 outputs averaged over the GEOS-Chem grid cell encompassing the APHH-Beijing sampling site.

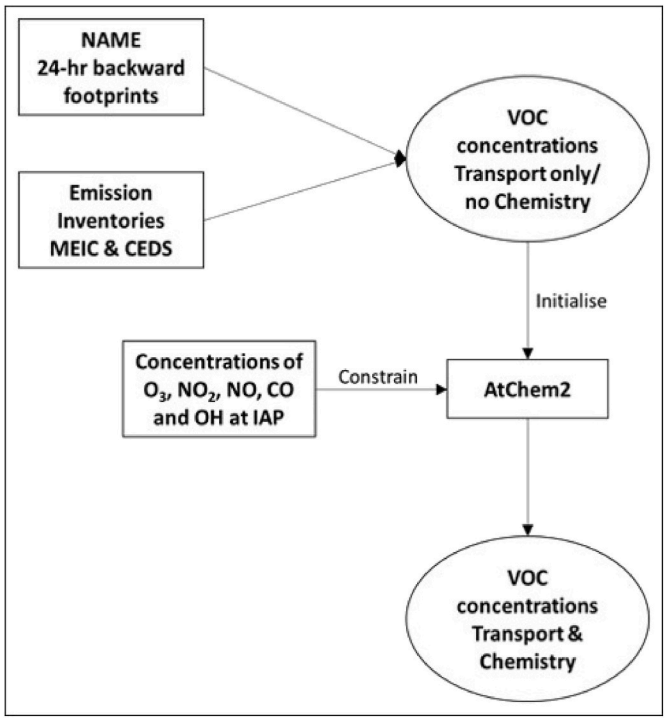

Fig. 2. AtChem2 combined with NAME dispersion footprints (NAME-AtChem2).

3. Results and discussions

3.1. VOC:CO ratios

Studies have suggested that the ratio between VOC and CO does not differ much from year to year and, therefore, that it can be used as a reliable predictor of the VOC levels. For example, in London the VOC/CO ratio for the majority of the VOC species did not change significantly during the 10 years from 1998 to 2007 (von Schneidemesser et al., 2010). Using this hypothesis, the average measured VOC/CO ratio for

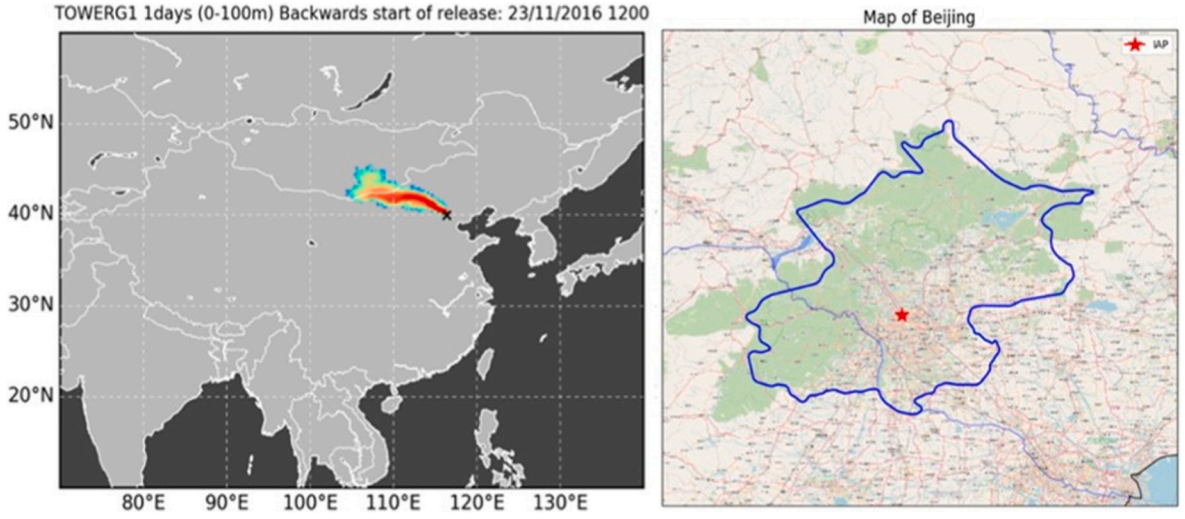

Fig. 1. Left: Example of a 24-h backwards NAME footprint arriving at the IAP meteorological tower during the winter campaign. Right: The extent of the Beijing area in blue. Base map and data are sourced from OpenStreetMap and its contributors (© OpenStreetMap, www.openstreetmap.org).

benzene and toluene in Beijing was calculated. Moreover, an average VOC/CO ratio was derived using VOC data from the literature (Li et al., 2015) and CO data from a nearby network station in Beijing (Shi et al., 2019) between 13 and 22 November 2014, as well as from the measurements taken in Beijing in November in 2016. The derived ratios are very similar between the two years, with benzene/CO ratios of 0.92 and 1.06 and toluene/CO ratios of 1.13 and 1.10 in 2014 and 2016, respectively. These derived ratios were multiplied by the measured CO (from APHH) in 2016 to investigate whether they could be used to predict VOC levels and daily variations. In addition, the measured ratios from November 2016 were multiplied by modelled CO using NAME and emission inventories (Panagi et al., 2020) to provide an additional comparison.

As shown in Fig. 3, during the winter campaign the measured VOC/CO ratio captures the VOC concentrations and variations well. Using the ratio for each year, the correlation coefficients of benzene measurements from the campaign with the measured benzene/CO ratio from 2014 to 2016 result in an $r = 0.98$ and for the toluene measurements an $r = 0.91$ with the measured toluene/CO ratio from 2014 to 2016. Furthermore, the correlation coefficients from the measured VOC/modelled CO are $r = 0.83$ for benzene and $r = 0.82$ for toluene. The VOC/CO ratio technique can be helpful in understanding the VOC levels in situations where there are no available measurements, although long term and more detailed VOC measurements in Beijing would be necessary to investigate this further. Furthermore, a decent estimate of VOC levels for the measurement period in Beijing can be obtained by using the CO modelled using the NAME footprints and the emission inventories with a VOC/CO ratio to provide information on the VOC concentrations if data is not available.

3.2. *Modelling air masses, the emissions of VOCs and sectoral contributions to Beijing*

The pathways of the air masses and the regions the air masses travelled over are important to understand how the air masses are influenced by the pollution emissions from those regions, as well as how the pollution is transported (Donnelly et al., 2016). Some regions are more polluted than others, which can lead to more pollution being transported to Beijing from those regions (M. Li et al., 2019). To investigate the pathways of air masses arriving at Beijing from the NAME model, the domain was separated into four quadrants (North-West (N-W), North-East (N-E), South-West (S-W) and South-East (S-E), see Fig. 4). The four quadrants intersect at the Institute of Atmospheric Physics (IAP) meteorological tower where the measurements for the APHH campaign took place.

In Fig. 4, the air mass distributions for the winter campaigns are presented. During the 2016 campaign, the air masses spent more time over the regions north of Beijing (64 %). For a large amount of the time (36 %) the air masses spent time over the south which has considerably higher density of anthropogenic sources in the regions south of Beijing: as an example, Fig. 4 shows that the emissions of toluene from industrial sources are largely concentrated in the SW and SE quadrants. It is therefore important to study the air masses arriving at Beijing from the south, as these can affect the pollution transported to Beijing, which reveals the importance and need for stricter control measures in different areas in different seasons (Panagi et al., 2020).

Using the NAME footprints combined with the VOC emission inventories, it is possible to model the sectoral contributions and transportation of VOCs from different source regions to Beijing. Fig. 5 shows the sectoral and spatial contributions from sources emitted within Beijing and sources emitted and transported from outside Beijing within 1 day of air mass travel. This enables local contributions to be

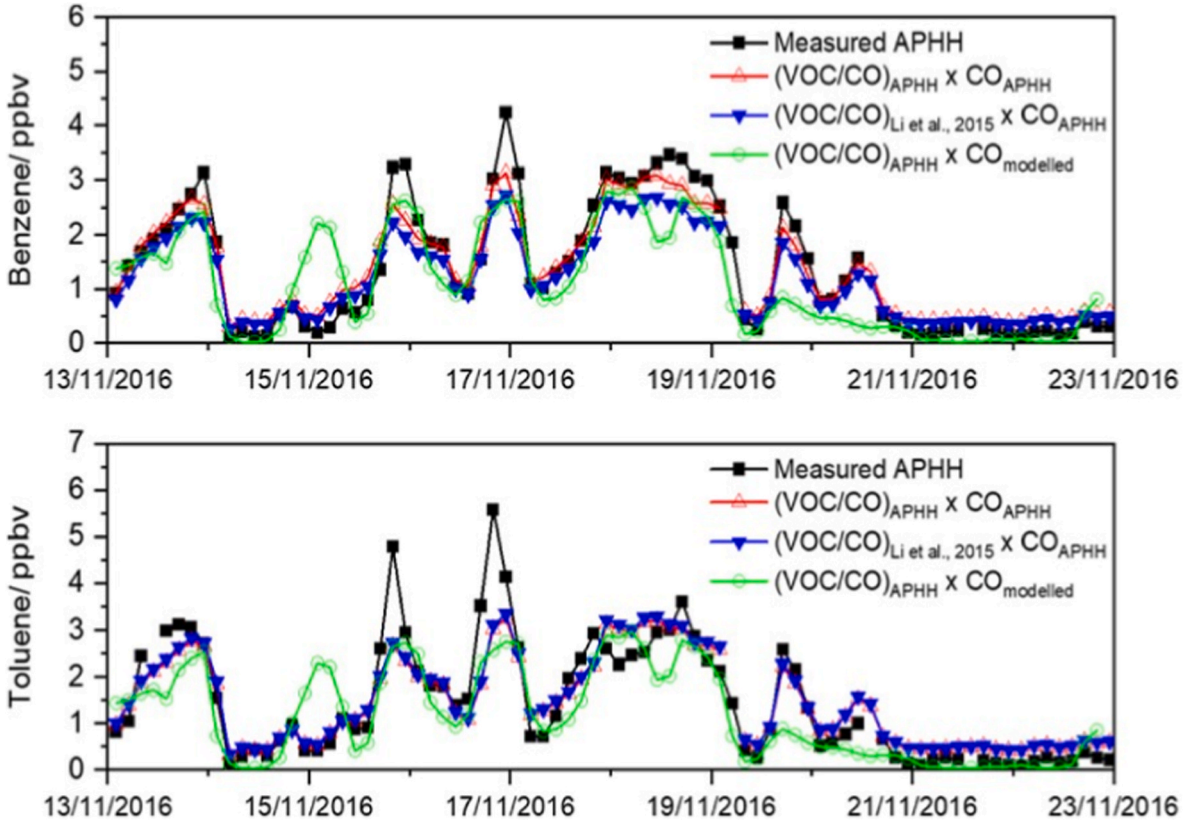

Fig. 3. The relationship between VOCs measured during the winter APHH campaign, calculated from the measured VOC/CO ratio during 2016 (averaged over the campaign period) and 2014 (from Li et al., 2015) and multiplication by the CO measured during the campaign.

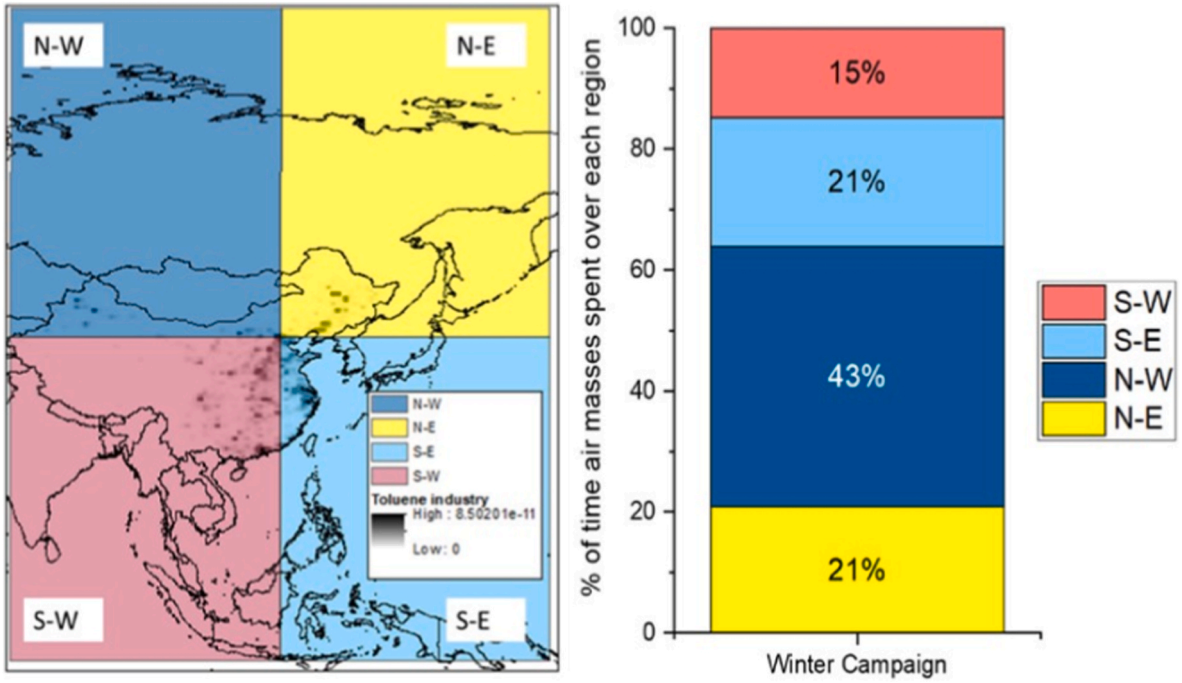

Fig. 4. The four quadrants used to investigate the air mass pathways distribution and to the right, the percentage of air mass pathways distribution over the four quadrants during the campaign. On the map, the industrial toluene emissions (kg mˆ2 sˆ(-1)) from.

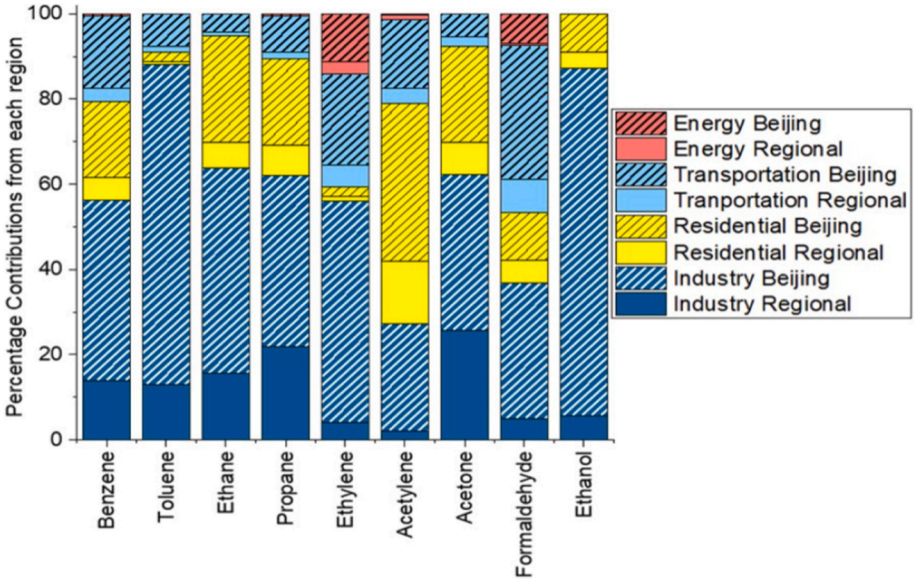

Fig. 5. VOC contributions (in percentages) from each emission sector from Beijing and the surrounding region.

distinguished from regional contributions, by sector.

During the campaign, approximately 80 % of the VOCs affecting the levels in Beijing are emitted from local sources (i.e., within the city) and the remaining 20 % from sources outside of Beijing within the 24-h air mass travel period. The largest contributors from outside Beijing during the winter campaign were the industrial emissions of acetone, propane, ethane, toluene and benzene, and residential regional emissions of acetylene. During the one-day runs, the contributions to Beijing from propane and acetone were highest from outside of Beijing. The results from the emission inventories and the air mass pathways suggest that industrial sources to the south of Beijing and within Beijing are very important drivers of the VOC levels in Beijing in winter.

3.3. How VOC levels are affected by chemical evolution

The results obtained using NAME together with the emission inventories are based on the (unrealistic) assumption that there is no impact of oxidative chemistry during the 24 h travel of an air mass. In order to investigate the effect of the chemistry, the AtChem2 box-model was initialized with the VOC concentrations modelled by coupling NAME with the emission inventories (see Section 2.3). Since observations are only available at the point of arrival (the IAP tower in Beijing), the box model assumes that NO_x and O_3 (and therefore OH) are homogeneous along the entire trajectory: this assumption is unlikely to be true, and for this reason, the model was run under three different scenarios as outlined below. These scenarios are used to investigate how the

assumptions about the NO_x, O_3, and OH levels affect the VOC concentration during the 24-h transport pathways:

- S1: Constrained to measurements of O_3, NO_2, NO, CO at the IAP tower. This is the base scenario and assumes that O_3, NO_x, and CO are the same along the trajectory as in Beijing.
- S2: Constrained to measurements of NO_2, NO, CO, and to double the O_3 measured at the IAP tower – to observe how higher ozone levels along the trajectory affect the chemistry.
- S3: Constrained to OH measurements only – to account for any underestimation of OH in the previous scenarios compared to the measured OH at IAP.

The results of the different simulation scenarios were compared against the measurements of each VOC at the IAP tower in Beijing during the winter campaign. The mean measured and modelled concentrations for each VOC species are shown in Table 1. The majority of the VOC emissions were underestimated in the emission inventories, except the toluene concentrations, which were overestimated (Acton et al., 2020). The measured and modelled datasets were normalized by their mean (campaign average) for ease of visualization and to remove the bias caused by overestimations/underestimations of emissions, as presented in Fig. 6.

It is observed that during the winter APHH campaign, the modelled concentrations calculated with NAME + emission inventories, and the ones calculated with the AtChem2 chemical box model, are well correlated, and therefore this approach can be considered able to predict observed VOC variability.

The correlation coefficients of the measured vs. modelled VOC species can be used to quantify how well the trajectories capture the emissions affecting Beijing and whether there is any impact from chemistry. During the winter campaign, the correlation coefficients of the measured vs. the modelled VOCs with no chemistry involved (i.e., calculated using just NAME with the emission inventories) show a good agreement for all species with correlation coefficients in the range of r = 0.82–0.89, with ethanol showing the lowest correlation (r = 0.76).

The differences in the VOC correlation coefficients between each scenario indicate how species are affected by loss and formation of secondary products from VOC oxidation in Beijing. When chemistry was introduced using the box model, the correlation coefficients increased slightly for all species in the range of r = 0.84–0.91 for scenarios S1 and S2, except for acetone and formaldehyde. In scenario S3, where OH is at higher levels (OH measured at the IAP tower in Beijing), the correlation coefficients decreased to r = 0.4–0.88. The decrease in correlation in the higher OH scenario was due to the faster loss of VOCs via reaction with OH. The most significant decreases were observed for toluene and ethene, which are the most reactive species among the hydrocarbons investigated. On the other hand, the correlation coefficient of acetone and formaldehyde decreased to r = 0.45 and r = 0.32, respectively (scenario S1), and increased as OH levels rose to r = 0.80 and r = 0.87, respectively (scenario S3).

During the winter campaign, scenario S3 (where OH was constrained to the measurements and not calculated from the model, and was therefore higher) led to higher loss of hydrocarbon species, with the smallest effects for ethane and benzene (approximately 5 % and 20 %, respectively), and the highest effects for toluene and ethene (approximately 63 % and 75 %, respectively). In this scenario, for photochemically produced OVOCs such as acetone and formaldehyde, an increase in production of approximately 650 % and 3500 %, respectively, was observed compared to the NAME scenario without any chemistry.

Finally, the relationship between NO_x, VOCs, and O_3 for the measurements and for the S1 base scenario was investigated to determine whether the modelled VOCs follow the same relationship as the measured VOCs. Fig. 7 presents scatterplots of NO *x* vs. VOCs, color-coded by the mixing ratio of O_3 to investigate differences. During the winter campaign, the model follows the same relationship as the measured VOCs (Fig. 7): O_3 is higher when NO_x and VOC levels are low. Moreover, it is observed that VOCs are highly correlated with NO_x, indicating that NO_x and VOCs are possibly emitted from similar sources. Both the results from the model and the measurements show similar relationships (same dependence on NO_x and O_3) for the aliphatic and the aromatic VOCs, while the relationship of the OVOCs between the model and the measurements is not as strong because OVOCs are secondary products, and the assumptions made by the model regarding the variability of O_3, NO_x, and OH along the trajectory of the air mass cannot fully capture OVOC production.

Table 1
Average concentrations of measured and modelled VOCs (ppbv) from a series of scenarios to assess the impact of chemical processing on modelled VOCs, and the O_3, NO_x, and OH concentrations constrained in the model runs.

VOC	Measured[a]	NAME[b]	S1[c]	S2[d]	S3[e]
Benzene	1.5	2.1	2.1	2	1.7
Toluene	1.7	7.8	7.1	6.8	2.9
Ethane	8.6	3.4	3.4	3.4	3.2
Propane	6	3.7	3.6	3.6	3
Ethene	6.9	5.1	4.4	4.1	1.3
Acetylene	5.3	2	2	2	1.7
Ethanol	11.7	6.5	6.1	5.9	3.6
Acetone	7.2	0.6	1	1.2	3.9
Formaldehyde	1.9	0.8	7.9	10.2	27.4
O_3/ppbv	–	–	8.9	17.8	8.8
NO_x/ppbv	–	–	71.9	72.0	72.6
OH/molecule cm^{-3}	–	–	1.4 E+05	2.0 E+05	2.3 E+06

[a] Mean campaign VOC average.
[b] Modelled values from the combination of MEIC and NAME.
[c] S1: Constraining original measurements (O 3, NO 2, NO, CO measured at the IAP tower) in NAME-AtChem2 runs.
[d] S2: Constraining original measurements and doubling O 3 in NAME-AtChem2 runs.
[e] S3: Constraining OH measurements only in NAME-AtChem2 runs.

3.4. Formaldehyde production

Formaldehyde is mainly a secondary product and the most abundant oxygenated volatile organic compound (OVOC). As indicated by the model results (see Table 1), the formaldehyde concentration rapidly increases through photochemical reactions in the first 24 h of transport, in addition to its direct emissions. Through photolysis, formaldehyde leads to the production of hydroxyl (OH) and hydroperoxy radicals (HO_2), which drive O_3 production (Calvert et al., 2015).

To better understand the role of chemistry on the concentrations of formaldehyde and how formaldehyde is produced in the air masses traveling to Beijing, additional runs of the AtChem2 box model were made with anthropogenic formaldehyde emissions set to zero for all scenarios. In these runs, the model used a chemical mechanism containing only inorganic chemistry and methane (set to a constant concentration of CH_4 at 1.989 ppm), with no other VOCs present. These tests estimate the amount of formaldehyde produced by the oxidation of CH_4 and allow for the calculation of the amount of formaldehyde produced from the reactions of the other VOCs with OH (by subtracting the anthropogenic formaldehyde measured with NAME and the formaldehyde produced by CH_4 from the total formaldehyde reported in each scenario), within 24 h of travel from Beijing (Table 2).

Fig. 8 presents the percentages of formaldehyde production in three categories during each scenario. The three categories are production via production by oxidation of CH_4, production by oxidation of other VOCs and production directly from anthropogenic sources. The major source of formaldehyde is secondary formed formaldehyde, produced by the oxidation of the other VOCs investigated in this study. During the winter campaign, formaldehyde produced by CH_4 oxidation is less than 1 % for all scenarios except S3 (approximately 8 %).

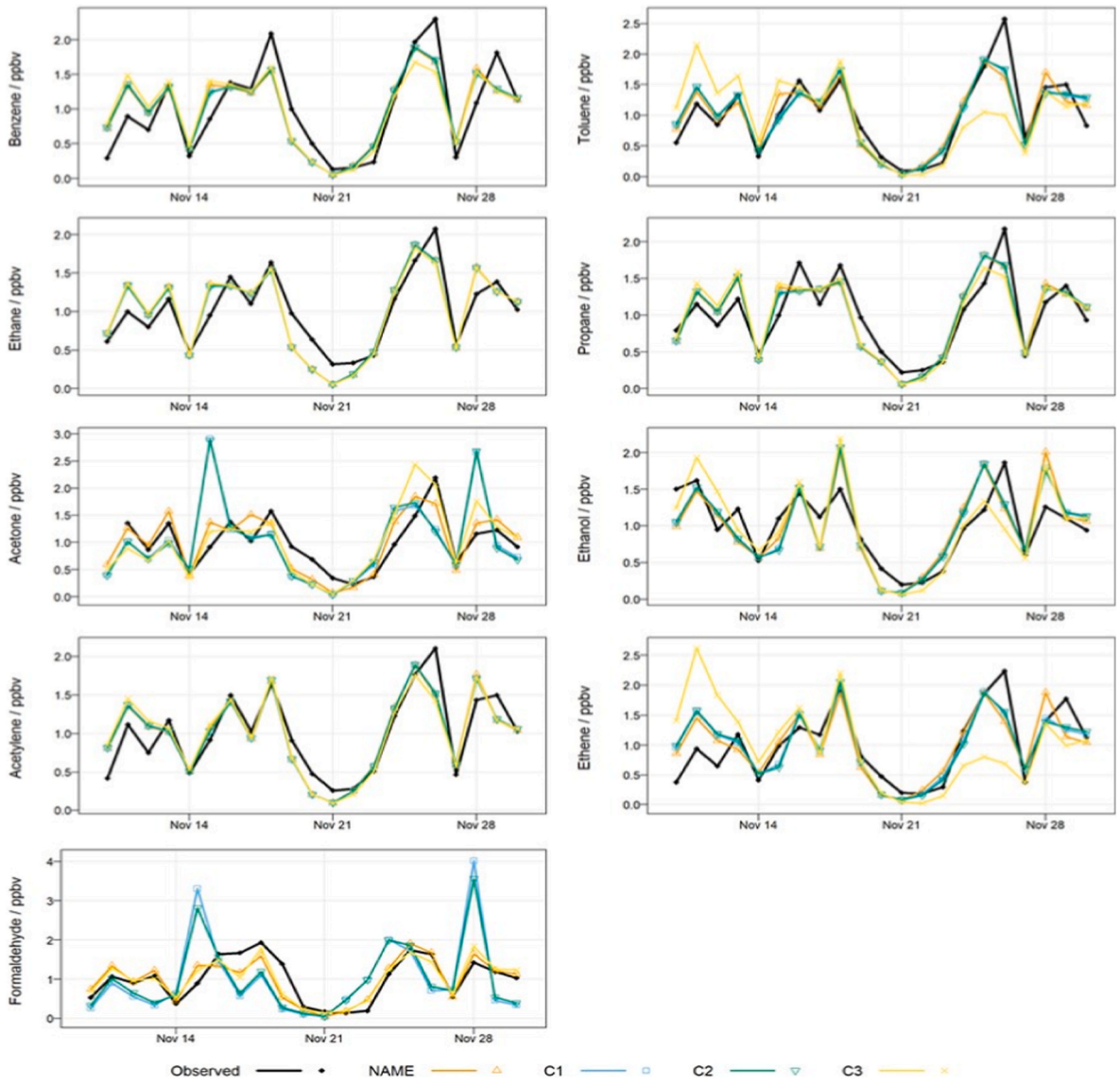

Fig. 6. Normalized plots from the five modelled scenarios vs. measured VOC concentrations during the winter campaign (scenarios are detailed in Table 1).

3.5. Ozone formation potential (OFP)

The production of O_3 can be limited either by the availability of VOCs or by the availability of NO_x, and studies show that the O_3 increase in China is largely related to the increase in VOC emissions, with different species having different contributions to O_3 formation (Cheng et al., 2010; Geng et al., 2009; Li et al., 2020). Therefore, to understand the ozone formation potential of the mixture arriving at Beijing, the ozone formation potential (OFP) was calculated using the concentrations of the reacted modelled and measured VOCs (in μg m^{-3}) and the Maximum Incremental Reactivity (MIR). The equation for calculating OFP is:

$$OFP_i = MIR_i \; x \; VOC_i$$

The MIR is different for each species and represents the amount of ozone formed per gram of VOC (g O_3/g VOC) (Carter, 1994). In Table 3, the calculated MIR is summarized as the total O_3 production potential for all NMVOCs and for all OVOCs in the model.

It is observed that scenario S3 (OH measurements constrained) has the lowest overall ozone formation potential for the NMVOCs, because the high OH decreases the concentrations of VOCs, which decreases the formation of O_3 in a VOC-limited environment (Table 3). Toluene and ethylene have the highest OFP for the NMVOCs throughout all the scenarios. For the OVOCs, S3 has the highest OFP, especially for formaldehyde. As observed earlier, OVOCs have low anthropogenic emissions but are very rapidly produced in the atmosphere by photochemical reactions, and then through photolysis, they produce new hydroxyl (OH) and hydroperoxy radicals (HO_2), which in turn drive O_3 production.

3.6. Comparison of NAME-AtChem2 to GEOS-Chem

The GEOS-Chem model was utilized to evaluate the simplified methodologies implemented in the NAME and NAME-AtChem2 models. These simplified approaches were compared against the comprehensive chemical transport model in GEOS-Chem, which accounts for all relevant chemical and physical processes. Table 4 compares the results of the runs with NAME-AtChem2 with daily 24-h mean surface VOC concentrations from GEOS-Chem and the VOC measurements.

The results show that GEOS-Chem observed benzene and toluene concentrations similar to the NAME-AtChem2 S1 – S2 scenarios. The overestimations of aromatics in GEOS-Chem could possibly be due to underestimations in OH and in the oxidation rates of these VOCs (Miller et al., 2016), similar to the overestimations of NAME-AtChem (S1 – S2) when OH was underestimated. NAME-AtChem2 overestimates

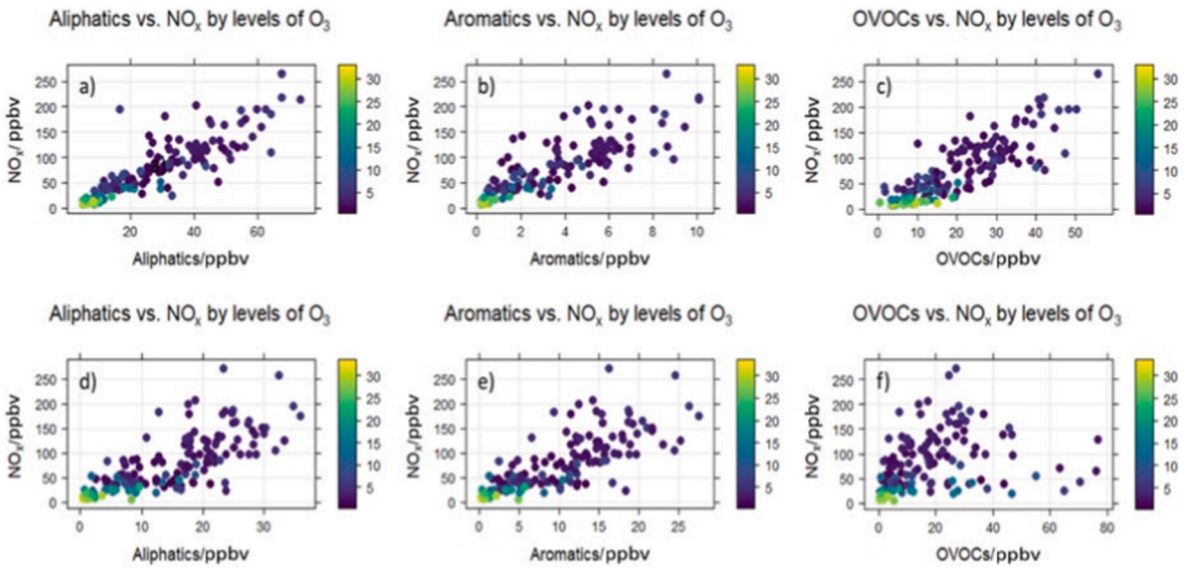

Fig. 7. NO_x/VOC relationship with O_3 levels (color bar in ppbv) during the winter campaign, (a–c): measured VOCs, (d–f): modelled VOCs (S1).

Table 2
Average concentrations of formaldehyde produced via different processes in each model scenario (units in ppbv).

	CH_4 Oxidation	NMVOCs Oxidation	Anthropogenic Emissions
S1[a]	0.04	7.07	0.76
S2[b]	0.09	9.31	0.76
S3[c]	2.15	24.43	0.76

[a] S1: Constraining original measurements (O 3, NO 2, NO, CO measured at the IAP tower) in NAME-AtChem2 runs.
[b] S2: Constraining original measurements and doubling O 3 in NAME-AtChem2 runs.
[c] S3: Constraining OH measurements only in NAME-AtChem2 runs.

formaldehyde by 2–8 times (S1 – S3) and has a greater underestimate in ethanol in scenario S3. Both GEOS-Chem and NAME-AtChem2 underestimate ethane by 3.5 times and approximately 2.5 times, respectively.

Owing to large differences between the modelled mean values from each model and consistency in day-to-day variability, the daily values were normalized by their mean (average concentration during the study period for each species individually – November 2016) for visualization purposes and compared to the measured VOCs to investigate whether the models agree with the observed patterns and sources affecting VOCs in Beijing (Fig. 9). The greatest correlation between GEOS-Chem and NAME-AtChem2 daily means was for the S3 scenario, with ethanol, benzene, and propane showing the highest correlations of 0.67, 0.63, and 0.64, respectively.

As observed from the comparison of the modelled runs with the measured VOCs, both GEOS-Chem and NAME-AtChem2 methods can broadly capture the daily variation in the VOC concentrations from the use of monthly emission inventories. GEOS-Chem uses emission inventories to derive the NO_x and O_3 concentrations at each grid, while NAME-AtChem2 uses measured data from a single point and assumes concentrations are the same throughout the footprints, which can explain some of the discrepancies in the modelled concentrations between each method. Furthermore, the resolution of the GEOS-Chem simulations is coarser compared to the NAME-AtChem2 runs. Last but not least, the chemistry schemes used in the two models are different, which can also result in some differences in the modelled concentrations.

3.7. Comparison with recent studies

Ambient conditions in Beijing have changed since the 2016 APHH campaign, following extensive control measures. Post-2016 studies in Beijing (Li et al., 2023; Liu et al., 2023, 2024; Cui et al., 2022) reported substantial reductions in total VOC concentrations but a largely unchanged wintertime source structure and photochemical regime. Li et al. (2023) observed a 63 % decrease in VOC levels between 2015 and 2019, with the sharpest declines in combustion-related hydrocarbons, while solvent- and aromatic-related compounds remained important. Liu et al. (2024) found that vehicle exhaust, LPG/NG use, and coal combustion continue to dominate VOC emissions through 2020, and that Beijing's atmosphere remains predominantly VOC-limited. Similarly, Cui et al. (2022) and Liu et al. (2023) showed that vehicle, solvent, and industrial sources prevail during winter, with VOC-limited chemistry at urban sites and mixed sensitivity in industrial areas. These studies indicate that the dominant processes observed in this study remain characteristic of present-day wintertime conditions in Beijing.

4. Conclusions

In this study, we investigated the capability to model VOC concentrations in Beijing during the winter APHH campaign (from 10th of November to 31st of November 2016) using a number of different approaches and explored the effects that NO_x and O_3 levels have on VOC concentrations and the effect of VOC concentrations on O_3 formation. The production of formaldehyde was also investigated in this study.

Initially, modelled CO was used to calculate VOCs using the average measured VOC/CO ratio. The results indicate that one can reasonably predict VOC concentrations by multiplying the measured ratio by CO. However, there are limitations to this method as a long VOC dataset is needed to confirm that the relationship holds over longer time periods. This technique can, however, be used for a rapid understanding of VOC levels when VOC and CO measurements are not present by using just CO emission inventories and the NAME model with the measured VOC/CO of previous years.

Another approach is to combine the footprints calculated with the NAME dispersion model with the emission inventories and use the resulting VOC levels as inputs to inform the AtChem2 chemical box model, in order to estimate the impact of chemical processing on the composition of air masses during transport into Beijing. During the campaign period, this method was able to capture the variations in VOC

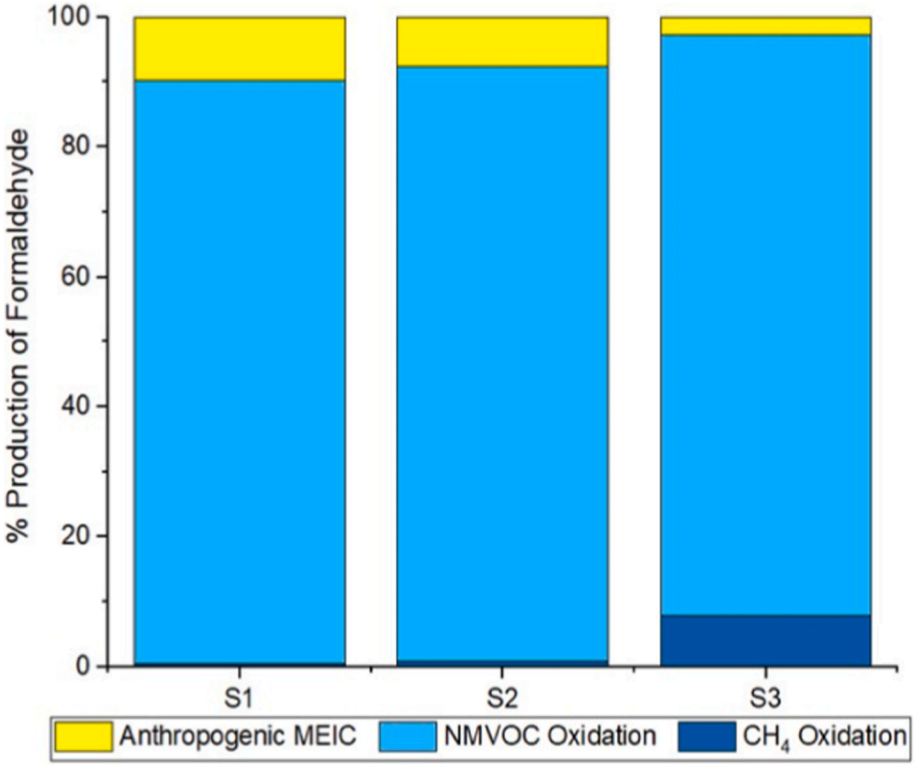

Fig. 8. Relative production of formaldehyde via different processes during the campaign.

Table 3
OFP from each scenario (μg m^{-3} of O_3).

VOC	S1[a]	S2[b]	S3[c]
Benzene	1.47	1.4	1.19
Toluene	28.4	27.2	11.6
Ethane	1.02	1.02	0.96
Propane	1.8	1.8	1.5
Ethylene	39.6	36.9	11.7
Acetylene	2	2	1.7
NMVOCs Total	**74.29**	**70.32**	**28.65**
Ethanol	9.15	8.85	5.4
Acetone	0.4	0.48	1.56
Formaldehyde	75.05	96.9	260.3
OVOCs Total	**84.6**	**106.23**	**267.26**

[a] S1: Constraining original measurements (O_3, NO_2, NO, CO measured at the IAP tower) in NAME-AtChem2 runs.
[b] S2: Constraining original measurements and doubling O_3 in NAME-AtChem2 runs.
[c] S3: Constraining OH measurements only in NAME-AtChem2 runs.

Table 4
Average concentrations from NAME-AtChem2 scenarios, GEOS-Chem, and measured VOCs during the winter campaign (units in ppbv).

VOC	Measured[a]	GEOS-Chem[b]	NAME[c]	S1[d]	S2[e]	S3[f]
Benzene	1.5	2.1	2.1	2.0	2.0	1.7
Toluene	1.7	6.1	7.8	7.0	6.8	2.9
Ethane	8.6	2.5	3.4	3.0	3.4	3.2
Propane	6.0	3.7	3.7	4.0	3.6	3.0
Acetone	7.2	1.3	0.6	1.0.	1.2	3.9
Formaldehyde	1.9	3.3	0.8	8.0	10	27.0
Ethanol	11.7	4.1	6.5	6.0	5.9	3.6

[a] Mean campaign VOC average.
[b] Modelled values from GEOS-Chem simulations.
[c] Modelled values from the combination of MEIC and NAME.
[d] S1: Constraining original measurements (O_3, NO_2, NO, CO measured at the IAP tower) in NAME-AtChem2 runs.
[e] S2: Constraining original measurements and doubling O_3 in NAME-AtChem2 runs.
[f] S3: Constraining OH measurements only in NAME-AtChem2 runs.

concentrations well compared with the measurements. Moreover, the method is in good agreement with the results of the GEOS-Chem chemical transport model, revealing the importance of understanding how using different parameters in the modelling of chemical processes can affect the results and how this can subsequently affect policymaking. In particular, the two methods (NAME + AtChem2 and GEOS-Chem) show differences in the modelled concentrations of chemical species investigated in this study due to their different approaches, which could lead to different policy decisions being taken.

Through the combination of NAME, emission inventories, and AtChem2, it was determined that the majority of the emissions affecting VOC levels in Beijing are from local sources, and their concentrations are largely controlled by the chemistry in Beijing. One of the limitations of coupling NAME with the AtChem2 box model is the assumption of homogeneous "pollution" along the entire transport pathway. This assumption is not realistic when considering long-range transport owing to varying atmospheric conditions and emission sources along the travel pathways; therefore, the model was run under three different scenarios to evaluate the sensitivity of the results to the model assumptions. Within one day of travel, and when the majority of sources affecting that period are local, the model scenarios can help understand how different atmospheric conditions can affect VOC levels not only in Beijing but also in other regions around the world. The three scenarios suggest that OH levels dominate the chemistry of the species, with higher OH revealing higher loss (for hydrocarbons) and production (for OVOCs) of the VOC species. Furthermore, higher OH will decrease transport from outside of Beijing since the loss of VOCs will occur faster before they arrive in Beijing. The highest impact of high OH levels was on ethene and toluene, with a decrease in their concentrations of approximately 63 % and 75 %, respectively. However, high OH was also associated with the highest production of OVOCs, such as acetone and formaldehyde, which

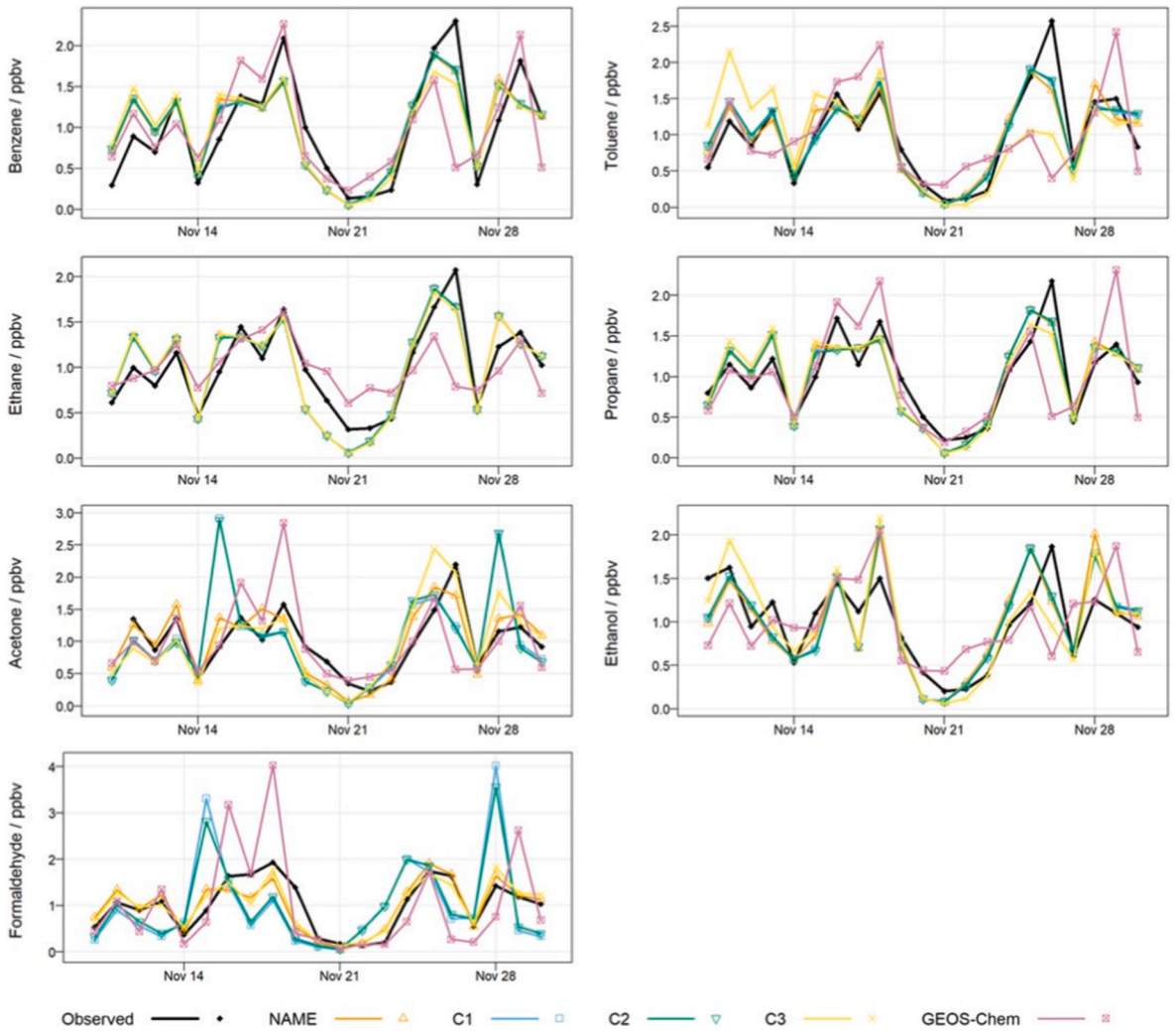

Fig. 9. Comparison of day-to-day variability in observed and modelled VOCs. Normalized by mean (November 2016) time series of NAME without chemistry (NAME), NAME-AtChem2 (S1 – S3) vs GEOS-Chem vs measured VOC during the winter campaign.

increased by approximately 550 % and 3500 %, respectively, within the first 24 h after they were emitted, compared to the concentrations calculated with no chemistry.

The production of formaldehyde was further investigated in this study, and it was determined that the majority of formaldehyde is produced from the oxidation of NMVOCs in the atmosphere. The O_3 formation potential was calculated to determine that species such as formaldehyde, ethene, and toluene are the highest contributors to ozone formation potential due to their higher maximum incremental reactivities; therefore, at high concentrations of these three species, the OFP increases. Reducing the concentrations of the VOCs investigated in this study will lead to a decrease in formaldehyde concentrations, which will further decrease O_3 formation.

For more effective control of VOCs and, consequently, O_3 in Beijing, the combination of NAME with emission inventories suggests that industrial sources need to be more effectively regulated within and outside Beijing since they lead to the highest pollution events in Beijing. Future work is needed that includes biogenic VOCs along with anthropogenic VOCs to gain a better understanding of the effect of biogenic VOCs on VOC levels and atmospheric chemistry in Beijing. Finally, more accurate emission inventories are needed to reduce uncertainties for deriving policy controls. This study is based on a three-week long campaign, and captures the dominant wintertime processes, but not the full seasonal or inter-annual variability. Longer-term and multi-site measurements, such as those of Li et al. (2023) and Liu et al. (2024), provide valuable context showing the persistence of the same emission patterns over subsequent years.

CRediT authorship contribution statement

Marios Panagi: Writing – review & editing, Writing – original draft, Visualization, Software, Methodology, Investigation, Formal analysis, Data curation, Conceptualization. **Roberto Sommariva:** Writing – review & editing, Software, Data curation, Conceptualization. **Zoë L. Fleming:** Writing – review & editing, Software, Data curation. **Paul S. Monks:** Writing – review & editing, Conceptualization. **Gongda Lu:** Writing – review & editing, Software. **Eloise A. Marais:** Writing – review & editing, Software. **James R. Hopkins:** Writing – review & editing, Data curation. **Alastair C. Lewis:** Writing – review & editing, Data curation. **Qiang Zhang:** Writing – review & editing, Software. **James D. Lee:** Writing – review & editing, Data curation. **Freya A. Squires:** Writing – review & editing, Data curation. **Lisa K. Whalley:** Writing – review & editing, Data curation. **Eloise J. Slater:** Writing – review & editing, Data curation. **Dwayne E. Heard:** Writing – review & editing, Data curation. **Robert Woodward-Massey:** Writing – review & editing, Data curation. **Chunxiang Ye:** Writing – review & editing, Data curation. **Joshua D. Vande Hey:** Writing – review & editing, Supervision, Conceptualization.

Declaration of competing interest

The authors declare that they have no known competing financial interests or personal relationships that could have appeared to influence the work reported in this paper.

Acknowledgments

We would like to thank the UK Met Office for supplying the Unified Model Meteorological data and the use of the NAME model and the CEDA for providing space on the JASMIN supercomputer to run the model. We thank the University of Leicester's High Performance Computing services for supplying the necessary computing power for plotting and storing the model output and Duncan Law-Green at the University of Leicester for developing the code to plot and interpret the NAME model output. Finally, we would like to thank the National Centre for Atmospheric Science (NCAS) and NERC for funding. GL thanks the PhD studentships funded by China Scholarship Council. J.D. Vande Hey acknowledges funding from the NIHR HPRU in Chemical Threats and Hazards at the University of Leicester. ES and RWM would like to thank the NERC SPHERES DTP for their PHD studentships.

Data availability

Atmospheric measurement data used in this study are available from the CEDA data archive at (Fleming et al., 2017). Dispersion model footprints are available from CEDA at (Panagi and Fleming, 2017). The modelled data in this study (modelled CO and air mass distribution) are available from the corresponding author upon request.

References

Acton, W.J.F., Huang, Z., Davison, B., Drysdale, W.S., Fu, P., Hollaway, M., Langford, B., Lee, J., Liu, Y., Metzger, S., Mullinger, N., Nemitz, E., Reeves, C.E., Squires, F.A., Vaughan, A.R., Wang, X., Wang, Z., Wild, O., Zhang, Q., Hewitt, C.N., 2020. Surface–atmosphere fluxes of volatile organic compounds in Beijing. Atmos. Chem. Phys. 20 (23), 15101–15125. https://doi.org/10.5194/acp-20-15101-2020.

Atkinson, R., 2000. Atmospheric chemistry of VOCs and NOx. Atmos. Environ. 34 (12–14), 2063–2101. https://doi.org/10.1016/S1352-2310(99)00460-4.

Brown, A., Milton, S., Cullen, M., Golding, B., Mitchell, J., Shelly, A., 2012. Unified modeling and prediction of weather and climate: a 25-Year journey. Bull. Am. Meteorol. Soc. 93 (12), 1865–1877. https://doi.org/10.1175/BAMS-D-12-00018.1.

Calvert, J.G., Orlando, J.J., Stockwell, W.R., Wallington, T.J., 2015. The Mechanisms of Reactions Influencing Atmospheric Ozone. Oxford University Press. https://doi.org/10.1093/oso/9780190233020.001.0001.

Carter, W.P.L., 1994. Development of ozone reactivity scales for volatile organic compounds. Air Waste 44 (7), 881–899. https://doi.org/10.1080/1073161X.1994.10467290.

Carter, W.P.L., Seinfeld, J.H., 2012. Winter ozone formation and VOC incremental reactivities in the Upper Green River Basin of Wyoming. Atmos. Environ. 50, 255–266. https://doi.org/10.1016/j.atmosenv.2011.12.025.

Cheng, H., Guo, H., Wang, X., Saunders, S.M., Lam, S.H.M., Jiang, F., Wang, T., Ding, A., Lee, S., Ho, K.F., 2010. On the relationship between ozone and its precursors in the Pearl River Delta: application of an observation-based model (OBM). Environ. Sci. Pollut. Control Ser. 17 (3), 547–560. https://doi.org/10.1007/s11356-009-0247-9.

Cryer, D.R., 2016. Measurements of Hydroxyl Radical Reactivity and Formaldehyde in the Atmosphere.

Cui, L., Wu, D., Wang, S., Xu, Q., Hu, R., Hao, J., 2022. Measurement report: ambient volatile organic compound (VOC) pollution in urban Beijing: characteristics, sources, and implications for pollution control. Atmos. Chem. Phys. 22 (18), 11931–11944. https://doi.org/10.5194/acp-22-11931-2022.

Donnelly, A., Naughton, O., Misstear, B., Broderick, B., 2016. Maximizing the spatial representativeness of NO 2 monitoring data using a combination of local wind-based sectoral division and seasonal and diurnal correction factors. J. Environ. Sci. Health Part A 51 (12), 1003–1011. https://doi.org/10.1080/10934529.2016.1198174.

Fleming, Z.L., Lee, J.D., Liu, D., Acton, J., Huang, Z., Wang, X., Hewitt, N., Crilley, L., Kramer, L., Slater, E., Whalley, L., Ye, C., Ingham, T., 2017. APHH: atmospheric measurements and model results for the atmospheric pollution & human health in a Chinese megacity. Centre for Environmental Data Analysis. https://catalogue.ceda.ac.uk/uuid/648246d2bdc7460b8159a8f9daee7844.

Geng, F., Cai, C., Tie, X., Yu, Q., An, J., Peng, L., Zhou, G., Xu, J., 2009. Analysis of VOC emissions using PCA/APCS receptor model at city of Shanghai, China. J. Atmos. Chem. 62 (3), 229–247. https://doi.org/10.1007/s10874-010-9150-5.

Giglio, L., Randerson, J.T., van der Werf, G.R., 2013. Analysis of daily, monthly, and annual burned area using the fourth-generation global fire emissions database (GFED4). J. Geophys. Res.: Biogeosciences 118 (1), 317–328. https://doi.org/10.1002/jgrg.20042.

Gu, Y., Li, Q., Wei, D., Gao, L., Tan, L., Su, G., Liu, G., Liu, W., Li, C., Wang, Q., 2019. Emission characteristics of 99 NMVOCs in different seasonal days and the relationship with air quality parameters in Beijing, China. Ecotoxicol. Environ. Saf. 169, 797–806. https://doi.org/10.1016/j.ecoenv.2018.11.091.

Guenther, A.B., Jiang, X., Heald, C.L., Sakulyanontvittaya, T., Duhl, T., Emmons, L.K., Wang, X., 2012. The model of emissions of gases and aerosols from nature version 2.1 (MEGAN2.1): an extended and updated framework for modeling biogenic emissions. Geosci. Model Dev. (GMD) 5 (6), 1471–1492. https://doi.org/10.5194/gmd-5-1471-2012.

Hopkins, J.R., Jones, C.E., Lewis, A.C., 2011. A dual channel gas chromatograph for atmospheric analysis of volatile organic compounds including oxygenated and monoterpene compounds. J. Environ. Monit. 13 (8), 2268. https://doi.org/10.1039/c1em10050e.

Hudman, R.C., Moore, N.E., Mebust, A.K., Martin, R.v., Russell, A.R., Valin, L.C., Cohen, R.C., 2012. Steps towards a mechanistic model of global soil nitric oxide emissions: implementation and space based-constraints. Atmos. Chem. Phys. 12 (16), 7779–7795. https://doi.org/10.5194/acp-12-7779-2012.

Jones, A., Thomson, D., Hort, M., & Devenish, B. (2007). The U.K. met office's next-generation atmospheric dispersion model, NAME III. In Air Pollution Modeling and its Application XVII (pp. 580–589). Springer US. https://doi.org/10.1007/978-0-387-68854-1_62.

Karl, T., Striednig, M., Graus, M., Hammerle, A., Wohlfahrt, G., 2018. Urban flux measurements reveal a large pool of oxygenated volatile organic compound emissions. Proc. Natl. Acad. Sci. 115 (6), 1186–1191. https://doi.org/10.1073/pnas.1714715115.

LaFranchi, B.W., Goldstein, A.H., Cohen, R.C., 2011. Observations of the temperature dependent response of ozone to NO x reductions in the Sacramento, CA urban plume. Atmos. Chem. Phys. 11 (14), 6945–6960. https://doi.org/10.5194/acp-11-6945-2011.

Li, J., Xie, S.D., Zeng, L.M., Li, L.Y., Li, Y.Q., Wu, R.R., 2015. Characterization of ambient volatile organic compounds and their sources in Beijing, before, during, and after Asia-Pacific Economic Cooperation China 2014. Atmos. Chem. Phys. 15 (14), 7945–7959. https://doi.org/10.5194/acp-15-7945-2015.

Li, J., Shi, Y., Wu, R., Xie, S., 2023. Variations of wintertime ambient volatile organic compounds in Beijing, China, from 2015 to 2019. Environ. Sci. Technol. Lett. 10 (2), 131–136. https://doi.org/10.1021/acs.estlett.2c00919.

Li, K., Jacob, D.J., Liao, H., Shen, L., Zhang, Q., Bates, K.H., 2019. Anthropogenic drivers of 2013–2017 trends in summer surface ozone in China. Proc. Natl. Acad. Sci. 116 (2), 422–427. https://doi.org/10.1073/pnas.1812168116.

Li, K., Jacob, D.J., Liao, H., Zhu, J., Shah, V., Shen, L., Bates, K.H., Zhang, Q., Zhai, S., 2019. A two-pollutant strategy for improving ozone and particulate air quality in China. Nat. Geosci. 12 (11), 906–910. https://doi.org/10.1038/s41561-019-0464-x.

Li, M., Zhang, Q., Kurokawa, J., Woo, J.-H., He, K., Lu, Z., Ohara, T., Song, Y., Streets, D. G., Carmichael, G.R., Cheng, Y., Hong, C., Huo, H., Jiang, X., Kang, S., Liu, F., Su, H., Zheng, B., 2017. MIX: a mosaic Asian anthropogenic emission inventory under the international collaboration framework of the MICS-Asia and HTAP. Atmos. Chem. Phys. 17 (2), 935–963. https://doi.org/10.5194/acp-17-935-2017.

Li, M., Zhang, Q., Zheng, B., Tong, D., Lei, Y., Liu, F., Hong, C., Kang, S., Yan, L., Zhang, Y., Bo, Y., Su, H., Cheng, Y., He, K., 2019. Persistent growth of anthropogenic non-methane volatile organic compound (NMVOC) emissions in China during 1990–2017: drivers, speciation and ozone formation potential. Atmos. Chem. Phys. 19 (13), 8897–8913. https://doi.org/10.5194/acp-19-8897-2019.

Li, Q., Su, G., Li, C., Liu, P., Zhao, X., Zhang, C., Sun, X., Mu, Y., Wu, M., Wang, Q., Sun, B., 2020. An investigation into the role of VOCs in SOA and ozone production in Beijing, China. Sci. Total Environ. 720, 137536. https://doi.org/10.1016/j.scitotenv.2020.137536.

Liu, C., Xin, Y., Zhang, C., Liu, J., Liu, P., He, X., Mu, Y., 2023. Ambient volatile organic compounds in urban and industrial regions in Beijing: characteristics, source apportionment, secondary transformation and health risk assessment. Sci. Total Environ. 855, 158873. https://doi.org/10.1016/j.scitotenv.2022.158873.

Liu, Y., Yin, S., Zhang, S., Ma, W., Zhang, X., Qiu, P., Li, C., Wang, G., Hou, D., Zhang, X., An, J., Sun, Y., Li, J., Zhang, Z., Chen, J., Tian, H., Liu, X., Liu, L., 2024. Drivers and impacts of decreasing concentrations of atmospheric volatile organic compounds (VOCs) in Beijing during 2016–2020. Sci. Total Environ. 906, 167847. https://doi.org/10.1016/j.scitotenv.2023.167847.

Liu, H., Liu, S., Xue, B., Lv, Z., Meng, Z., Yang, X., Xue, T., Yu, Q., He, K., 2018. Ground-level ozone pollution and its health impacts in China. Atmos. Environ. 173, 223–230. https://doi.org/10.1016/j.atmosenv.2017.11.014.

Liu, J., Mauzerall, D.L., Chen, Q., Zhang, Q., Song, Y., Peng, W., Klimont, Z., Qiu, X., Zhang, S., Hu, M., Lin, W., Smith, K.R., Zhu, T., 2016. Air pollutant emissions from Chinese households: a major and underappreciated ambient pollution source. Proc. Natl. Acad. Sci. 113 (28), 7756–7761. https://doi.org/10.1073/pnas.1604537113.

McDonald, B.C., de Gouw, J.A., Gilman, J.B., Jathar, S.H., Akherati, A., Cappa, C.D., Jimenez, J.L., Lee-Taylor, J., Hayes, P.L., McKeen, S.A., Cui, Y.Y., Kim, S.-W., Gentner, D.R., Isaacman-VanWertz, G., Goldstein, A.H., Harley, R.A., Frost, G.J., Roberts, J.M., Ryerson, T.B., Trainer, M., 2018. Volatile chemical products emerging as largest petrochemical source of urban organic emissions. Science 359 (6377), 760–764. https://doi.org/10.1126/science.aaq0524.

Miller, C., Jacob, D.J., González Abad, G., Chance, K., 2016. Hotspot of glyoxal over the Pearl River delta seen from the OMI satellite instrument: implications for emissions of aromatic hydrocarbons. Atmos. Chem. Phys. 16 (7), 4631–4639. https://doi.org/10.5194/acp-16-4631-2016.

Monks, P.S., Archibald, A.T., Colette, A., Cooper, O., Coyle, M., Derwent, R., Fowler, D., Granier, C., Law, K.S., Mills, G.E., Stevenson, D.S., Tarasova, O., Thouret, V., von

Schneidemesser, E., Sommariva, R., Wild, O., Williams, M.L., 2015. Tropospheric ozone and its precursors from the urban to the global scale from air quality to short-lived climate forcer. Atmos. Chem. Phys. 15 (15), 8889–8973. https://doi.org/10.5194/acp-15-8889-2015.

Monks, P.S., Granier, C., Fuzzi, S., Stohl, A., Williams, M.L., Akimoto, H., Amann, M., Baklanov, A., Baltensperger, U., Bey, I., Blake, N., Blake, R.S., Carslaw, K., Cooper, O.R., Dentener, F., Fowler, D., Fragkou, E., Frost, G.J., Generoso, S., von Glasow, R., 2009. Atmospheric composition change – global and regional air quality. Atmos. Environ. 43 (33), 5268–5350. https://doi.org/10.1016/j.atmosenv.2009.08.021.

Oram, D.E., Ashfold, M.J., Laube, J.C., Gooch, L.J., Humphrey, S., Sturges, W.T., Leedham Elvidge, E.C., Forster, G.L., Harris, N.R.P., Mead, M.I., Abu Samah, A., Phang, S.M., Chang-Feng, O.-Y., Lin, N.-H., Wang, J.-L., Baker, A.K., Brenninkmeijer, C.A.M., Sherry, D., 2017. A growing threat to the ozone layer from short-lived anthropogenic chlorocarbons. https://doi.org/10.5194/acp-2017-497.

Panagi, M., Fleming, Z.L., 2017. APHH: atmospheric dispersion model footprint plots made at the IAP-Beijing site during the summer and winter campaigns. Centre for Environmental Data Analysis. https://catalogue.ceda.ac.uk/uuid/88f3a3de77354692aeada98c5dad599b.

Panagi, M., Fleming, Z.L., Monks, P.S., Ashfold, M.J., Wild, O., Hollaway, M., Zhang, Q., Squires, F.A., vande Hey, J.D., 2020. Investigating the regional contributions to air pollution in Beijing: a dispersion modelling study using CO as a tracer. Atmos. Chem. Phys. 20 (5), 2825–2838. https://doi.org/10.5194/acp-20-2825-2020.

Parrish, D.D., Kuster, W.C., Shao, M., Yokouchi, Y., Kondo, Y., Goldan, P.D., de Gouw, J. A., Koike, M., Shirai, T., 2009. Comparison of air pollutant emissions among mega-cities. Atmos. Environ. 43 (40), 6435–6441. https://doi.org/10.1016/j.atmosenv.2009.06.024.

Rumchev, K., Brown, H., Spickett, J., 2007. Volatile organic compounds: do they present a risk to our health? Rev. Environ. Health 22 (1). https://doi.org/10.1515/REVEH.2007.22.1.39.

Saikawa, E., Kim, H., Zhong, M., Avramov, A., Zhao, Y., Janssens-Maenhout, G., Kurokawa, J., Klimont, Z., Wagner, F., Naik, V., Horowitz, L.W., Zhang, Q., 2017. Comparison of emissions inventories of anthropogenic air pollutants and greenhouse gases in China. Atmos. Chem. Phys. 17 (10), 6393–6421. https://doi.org/10.5194/acp-17-6393-2017.

Shi, Z., Vu, T., Kotthaus, S., Harrison, R.M., Grimmond, S., Yue, S., Zhu, T., Lee, J., Han, Y., Demuzere, M., Dunmore, R.E., Ren, L., Liu, D., Wang, Y., Wild, O., Allan, J., Acton, W.J., Barlow, J., Barratt, B., Zheng, M., 2019. Introduction to the special issue "In-depth study of air pollution sources and processes within Beijing and its surrounding region (APHH-Beijing).". Atmos. Chem. Phys. 19 (11), 7519–7546. https://doi.org/10.5194/acp-19-7519-2019.

Sillman, S., 1999. The relation between ozone, NOx and hydrocarbons in urban and polluted rural environments. Atmos. Environ. 33 (12), 1821–1845. https://doi.org/10.1016/S1352-2310(98)00345-8.

Slater, E.J., Whalley, L.K., Woodward-Massey, R., Ye, C., Lee, J.D., Squires, F., Hopkins, J.R., Dunmore, R.E., Shaw, M., Hamilton, J.F., Lewis, A.C., Crilley, L.R., Kramer, L., Bloss, W., Vu, T., Sun, Y., Xu, W., Yue, S., Ren, L., Heard, D.E., 2020. Elevated levels of OH observed in haze events during wintertime in central Beijing. Atmos. Chem. Phys. 20 (23), 14847–14871. https://doi.org/10.5194/acp-20-14847-2020.

Sommariva, R., Cox, S., Martin, C., Borońska, K., Young, J., Jimack, P., Pilling, M.J., Matthaios, V.N., Newland, M.J., Panagi, M., Bloss, W.J., Monks, P.S., Rickard, A.R., 2019. AtChem, an open source box-model for the master. Chemical Mechanism. https://doi.org/10.5194/gmd-2019-192.

Tang, X., Bai, Y., Duong, A., Smith, M.T., Li, L., Zhang, L., 2009. Formaldehyde in China: production, consumption, exposure levels, and health effects. Environ. Int. 35 (8), 1210–1224. https://doi.org/10.1016/j.envint.2009.06.002.

Uysal, N., Schapira, R.M., 2003. Effects of ozone on lung function and lung diseases. Curr. Opin. Pulm. Med. 9 (2), 144–150. https://doi.org/10.1097/00063198-200303000-00009.

von Schneidemesser, E., Monks, P.S., Plass-Duelmer, C., 2010. Global comparison of VOC and CO observations in urban areas. Atmos. Environ. 44 (39), 5053–5064. https://doi.org/10.1016/j.atmosenv.2010.09.010.

Wang, Y., Shen, L., Wu, S., Mickley, L., He, J., Hao, J., 2013. Sensitivity of surface ozone over China to 2000–2050 global changes of climate and emissions. Atmos. Environ. 75, 374–382. https://doi.org/10.1016/j.atmosenv.2013.04.045.

Warneke, C., de Gouw, J.A., Holloway, J.S., Peischl, J., Ryerson, T.B., Atlas, E., Blake, D., Trainer, M., Parrish, D.D., 2012. Multiyear trends in volatile organic compounds in Los Angeles, California: five decades of decreasing emissions. J. Geophys. Res. Atmos. 117 (D21). https://doi.org/10.1029/2012JD017899.

Whalley, L.K., Slater, E.J., Woodward-Massey, R., Ye, C., Lee, J.D., Squires, F., Hopkins, J.R., Dunmore, R.E., Shaw, M., Hamilton, J.F., Lewis, A.C., Mehra, A., Worrall, S.D., Bacak, A., Bannan, T.J., Coe, H., Percival, C.J., Ouyang, B., Jones, R.L., Heard, D.E., 2021. Evaluating the sensitivity of radical chemistry and ozone formation to ambient VOCs and NO x in Beijing. Atmos. Chem. Phys. 21 (3), 2125–2147. https://doi.org/10.5194/acp-21-2125-2021.

Yang, W., Zhang, Y., Wang, X., Li, S., Zhu, M., Yu, Q., Li, G., Huang, Z., Zhang, H., Wu, Z., Song, W., Tan, J., Shao, M., 2018. Volatile organic compounds at a rural site in Beijing: influence of temporary emission control and wintertime heating. Atmos. Chem. Phys. 18 (17), 12663–12682. https://doi.org/10.5194/acp-18-12663-2018.

Yao, Z., Shen, X., Ye, Y., Cao, X., Jiang, X., Zhang, Y., He, K., 2015. On-road emission characteristics of VOCs from diesel trucks in Beijing, China. Atmos. Environ. 103, 87–93. https://doi.org/10.1016/j.atmosenv.2014.12.028.

Zhang, Z., Zhang, Y., Wang, X., Lü, S., Huang, Z., Huang, X., Yang, W., Wang, Y., Zhang, Q., 2016. Spatiotemporal patterns and source implications of aromatic hydrocarbons at six rural sites across China's developed coastal regions. J. Geophys. Res. Atmos. 121 (11), 6669–6687. https://doi.org/10.1002/2016JD025115.

Zheng, B., Tong, D., Li, M., Liu, F., Hong, C., Geng, G., Li, H., Li, X., Peng, L., Qi, J., Yan, L., Zhang, Y., Zhao, H., Zheng, Y., He, K., Zhang, Q., 2018. Trends in China's anthropogenic emissions since 2010 as the consequence of clean air actions. Atmos. Chem. Phys. 18 (19), 14095–14111. https://doi.org/10.5194/acp-18-14095-2018.